Meccanica (2014) 49:2285–2297
DOI 10.1007/s11012-014-9974-1

Effect of ethanol addition on cyclic variability in a simulated spark ignition gasoline engine

A. K. Sen · A. Medina · P. L. Curto-Risso · A. Calvo Hernández

Received: 25 July 2013 / Accepted: 21 May 2014 / Published online: 28 June 2014

Abstract This study investigates the cycle-to-cycle variations (CCV) of heat release in a simulated spark ignition engine fueled by gasoline–ethanol blends. The equivalence ratio of the combustible mixture is changed from 0.7 to 0.9 and 1.0, i.e., from very lean to stoichiometric. Ethanol is added in the volumetric proportions of 5–25 %. For each equivalence ratio and for each ethanol fraction added, we calculate the coefficient of variation (COV) of the heat release time series. From the values of COV, we find that at a fixed equivalence ratio, the CCV of heat release decreases as the amount of ethanol addition is increased. We also find that for a fixed volume fraction of ethanol, the CCV increases with leaner mixtures. In addition, we use a continuous wavelet transform (CWT) to analyze the heat release time series. From the CWT, the dominant modes of the CCV are identified and the engine cycles over which these modes may persist are delineated. The results reveal that the CCV of heat release occur on multiple timescales and exhibit complex dynamics. With no ethanol added, high-frequency intermittent fluctuations together with more persistent low-frequency variations are observed. As the volume fraction of ethanol is increased, the low-frequency variations tend to become less persistent and more intermittent. Furthermore, at a fixed equivalence ratio, when ethanol fraction is increased, the overall spectral power is found to decrease significantly indicating that ethanol has a pronounced effect on reducing the CCV. An advantage of using a simulated model engine is that the computations can be easily carried out to a large number of cycles and thus determine the long term dynamics of the cyclic variations.

Keywords Cycle-to-cycle variations · Spark ignition engine · Gasoline–ethanol blends · Wavelet analysis

A. K. Sen
Department of Mathematical Sciences, Richard G. Lugar Center for Renewable Energy, Indiana University, 402 N. Blackford Street, Indianapolis, IN 46202, USA

A. Medina (✉) · A. Calvo Hernández
Departamento de Física de Aplicada, Universidad de Salamanca, 37008 Salamanca, Spain
e-mail: amd385@usal.es

P. L. Curto-Risso
Instituto de Ingeniería Mecánica y Producción Industrial, Universidad de la República, 11300 Montevideo, Uruguay

1 Introduction

In order to increase the thermal efficiency and reduce exhaust emissions of internal combustion engines, alternative fuels and fuel blends are increasingly being used, replacing conventional fuels such as gasoline and diesel [1, 2]. Ethanol can be produced from renewable energy sources such as agricultural feedstock, and it can be used as a supplemental fuel with

gasoline in a standard spark ignition engine without extensive modifications. The relative advantages and disadvantages of ethanol as a supplemental fuel have been discussed by many researchers. Among its advantages, ethanol has a higher octane number and a higher flame speed than gasoline. A higher octane number allows higher compression ratios to be used. Thus blending gasoline with ethanol will result in an increase in thermal efficiency and power output of the engine. The higher flame speed of ethanol will also lead to similar improvements. In addition, by virtue of higher octane number of ethanol, gasoline–ethanol blends will have better antiknock properties than gasoline. Ethanol addition has also been found to reduce the emissions of CO and unburned hydrocarbons. There have been several investigations, both experimental and theoretical, for studying the effect of ethanol addition to gasoline on engine performance and exhaust emissions [3–9].

The process variables such as pressure and heat release in an internal combustion engine undergo cycle-to-cycle variations (CCV) [10–14]. The CCV may become severe under lean-burn conditions, and for highly dilute mixtures with exhaust gas recirculation [11]. Cycle-to-cycle variations have been observed in spark ignition, compression ignition, and homogeneous charge compression ignition (HCCI) engines. The CCV may reduce the power output of the engine, lead to operational instabilities, and result in undesirable engine vibrations and noise. Several sources of CCV in a spark ignition engine have been identified. They include (a) turbulence intensity of the flow field in the cylinder, (b) variations in the fuel–air ratio, (c) amount of residual or recirculated exhaust gases in the cylinder, (d) spatial inhomogeneity of the mixture composition especially near the spark plug, and (e) spark discharge characteristics and flame kernel development [15–18]. It has been estimated that elimination of the CCV may lead to about 10 % increase in power output for the same fuel consumption in a gasoline engine [18]. There have been many studies on the analysis of the CCV in internal combustion engines. Some of these studies have revealed that any process that increases the burning velocity of the combustible mixture will result in a reduction of the CCV [19–21]. Because the burning velocity of ethanol-air mixture is higher than that of gasoline-air mixture [22], addition of ethanol to gasoline will reduce the CCV in a spark ignition engine.

For theoretical studies of the CCV, different types of combustion models have been developed by researchers. The so-called zero-dimensional model is based on purely thermodynamic considerations. The multi-dimensional models, on the other hand, are very detailed in their approach, and involve a system of partial differential equations which are numerically integrated on 2D or 3D geometric grids in the combustion chamber space [23–25]. Although the multi-dimensional models can provide very realistic information of the combustion process, with high spatial and temporal resolutions, their numerical simulation requires a large amount of computer storage and execution time.

In a recent paper, Curto-Risso et al. [26] developed a quasi-dimensional model of a gasoline engine. The quasi-dimensional model is derived from the assumption of a spherical flame front and the incorporation of two ordinary differential equations describing the evolution of the combustion process. It provides an improvement over the zero-dimensional model, and requires significantly less storage space and processing time than the multi-dimensional models. Their development is based on extensions of previous works on quasi-dimensional combustion models [27–32]. Using this quasi-dimensional model, Curto-Risso et al. [26] analyzed the time series of heat release variations in a gasoline engine, and validated their simulations by comparing the results with the experimental observations of Beretta [28]. More recently, Curto-Risso et al. [33] formulated a quasi-dimensional model for a spark ignition engine fueled by gasoline–ethanol blends, by incorporating the appropriate chemical reaction kinetics into their previous model [26]. This model was validated by comparing the model simulations with the experimental results of Bayraktar [9]. In particular, the model simulations obtained in [9] on power output, engine thermal efficiency, CO emission, and specific fuel consumption were shown to be in good agreement with the experimental results.

In the present work, using the model simulations of [33], we examine the cycle-to-cycle heat release variations in a spark ignition engine fueled by gasoline–ethanol blends. Our investigation is based on the coefficient of variation (COV), and wavelet analysis of the heat release time series. These analyses show that CCV decrease with increasing fractions of

ethanol, and that with regard to the fuel–air ratio, the CCV increase in going from stoichiometric to lean mixtures. In addition, the wavelet analysis describes the dominant modes of variability and delineates the engine cycles over which these modes may persist.

2 Combustion model, simulation scheme and validation

In our previous works [26, 31, 34], we developed a quasi-dimensional model for a gasoline engine. This model starts from the first principles of thermodynamics and includes the flow dynamics and chemical kinetics of the combustion process. It is based on the first principle of thermodynamics for open systems. The cylinder interior is considered as control volume and differential equations for pressure and temperature are stated for any engine stroke. During combustion a two-zone model is considered, thus distinguishing between unburned and burned gases. All gases are considered as ideal with temperature and pressure independent gas constant. The equivalence ratio is also taken as constant and, except in combustion, enthalpy changes are associated to temperature changes. The explicit shape of the differential equations for temperature and pressure, and other details can be found in [31]. The mass flow rates of the gases through the engine valves are quantified by the equations for a compressible flow through a flow restriction [11].

We use the turbulent combustion scheme proposed by Blizard and Keck [27] and later improved by Beretta [28]. The flame was assumed to be nearly spherical. It was further assumed that in the course of flame propagation, not all of the mass inside the flame is burned, but there are unburned eddies characterized by a typical length l_t. The evolution of the combustion process is governed by a set of coupled differential equations for the total mass within the flame front, m_e (unburned eddies plus burned gas), and burned mass, m_b.

$$\dot{m}_b = A_f \rho_u S_l + \frac{m_e - m_b}{\tau_b} \tag{1}$$

$$\dot{m}_e = A_f \rho_u \left[u_t \left(1 - e^{-\tau/\tau_b} \right) + S_l \right] \tag{2}$$

In these equations, a dot over a variable indicates a time derivative, and the subscripts u and b stand, for the unburned and burned gases, respectively; τ is the time from the start of combustion, and A_f is the area of the spherical flame front. This area is calculated from the radius, taking into account the volume of the gases inside the flame front: $V_f = V_b + (m_e - m_b)/\rho_u$, where $V_b = m_b/\rho_b$ is the volume of the burned gas mixture. The first term on the right hand side of Eq. (1) is associated with the laminar propagation of the flame front, and the second term represents burning of the mixture entrained within this flame front. The quantity $\tau_b = l_t/S_l$ is the characteristic time required for the combustion of a typical eddy of length, l_t, at the velocity S_l. In other words, τ_b represents the time that the flame front takes to develop into a turbulent flame from the initial laminar and spherical conditions [11]. Equation (2) describes the rate of change of the total gas mixture within the flame front at the velocity $u_t + S_l$ ($\tau \gg \tau_b$), where u_t is the characteristic (convective) velocity at which the fresh mixture crosses the flame front, and S_l is the laminar (diffusive) flame speed. The laminar combustion speed is determined from its reference value as [11]:

$$S_l = S_{l,0} \left(\frac{T_u}{T_{\text{ref}}} \right)^{\alpha} \left(\frac{p_u}{p_{\text{ref}}} \right)^{\beta} (1 - 2.06 y_r^{0.77}) \tag{3}$$

where y_r is the mole fraction of residual gases in the chamber and α, β are functions of the equivalence ratio [31]. The reference burning laminar speed, $S_{l,0}$, at reference conditions (T_{ref}, p_{ref}) is obtained from Gülder's model [22]. So, the laminar combustion speed depends on the equivalence ratio through α and β, and also on the mole fraction of residual gases from the previous cycle, y_r. Of course, in order to describe the overall combustion process, Eqs. (1–3) must be coupled to the thermodynamic ones for the pressure and the temperature inside the cylinder.

The simulation model was validated in [31] using pure isooctane as fuel. In this work the fuel considered is isooctane, C_8H_{18}, blended with ethanol, C_2H_5OH. The possible presence of water vapor in the reactants is taken into account. A fraction of the residual gases, y_r, is incorporated as reactants to the fresh mixture, so the combustion reaction can be written as:

$$\begin{aligned}
&(1 - y_r)(\varepsilon\varphi C_\alpha H_\beta O_\gamma N_\delta + 0.21 O_2 + 0.79 N_2 + f H_2O) \\
&+ y_r(v_1 CO_2 + v'_2 H_2O + v'_3 N_2 + v'_4 O_2 + v'_5 CO \\
&+ v'_6 H_2 + v'_7 H + v'_8 O + v'_9 OH + v'_{10} NO) \rightarrow v_1 CO_2 \\
&+ v_2 H_2O + v_3 N_2 + v_4 O_2 + v_5 CO + v_6 H_2 + v_7 H \\
&+ v_8 O + v_9 OH + v_{10} NO
\end{aligned} \tag{4}$$

Table 1 Geometrical and other parameters of the numerical simulation

Cylinder volume	7.63×10^{-4} m^3
Crank radius	60.0×10^{-3} m
Piston bore	90.0×10^{-3} m
Stroke-bore ratio	4/3
Spark-plug location	30.0×10^{-3} m
Compression ratio	7.75
Intake pressure	1.0×10^5 Pa
Intake temperature	293 K
Exhaust pressure	1.0×10^5 Pa
Exhaust temperature	600 K
Wall temperature	600 K
Spark advance	350°
Engine speed	1,044 rpm
Stroke	120 mm
Swept volume	763 cm^3

So, we consider 10 reaction products, that are incorporated as reactants to the following combustion process.

The ratio between the moles of water and dry air is denoted by f ($f = n_{H_2O}/n_{DA}$). For instance, if ethanol contains a mass fraction of water x_W and the mass fraction of ethanol in the blend is x_E:

$$f = \left(r_q \varphi \frac{x_W x_E}{1 - x_W x_E} \right) \frac{M_{DA}}{M_{H_2O}} \tag{5}$$

where M_{DA} and M_{H_2O} are the molecular weights of dry air and water respectively.

In order to validate the simulation for gasoline–ethanol blends we have considered the cylinder parameters of Bayraktar [7] (in that work some experimental measures for isooctane-ethanol blends up to 25 % ethanol by volume were presented). To complete the data required to simulate the model, we assume appropriate values for the dimensions and lift of the intake and exhaust valves. The values of the opening and closing times for the valves are fitted in order to get the same results of the engine performance for pure gasoline as found in [7] (see Tables 1 and 2).

Bayraktar's [7] experimental results for the engine efficiency (η), power output (P), CO emissions, and the specific fuel consumption (sfc) were reproduced for several volume fractions of ethanol. With respect to combustion, the laminar burning velocities estimated by Gulder [22] for ethanol-isooctane blends up to 25 % ethanol by liquid volume were used. We considered the same experimental evolution of the fuel/air equivalence ratio ϕ for the blend with the ethanol concentration that in [7] (the same interval from E0 to E12 is taken). Ethanol is an oxygenated fuel, so it has a high stoichiometric fuel–air ratio. Therefore, addition of ethanol to gasoline leads to leaner operation. The corresponding results are depicted in Fig. 1.

Table 2 Basic performance, consumption, and emission parameters used for calibration purposes

	Experimental [5]	Computed
Power (kW)	6.9	6.9
Efficiency (%)	22.5	22.2
sfc [kg/(kW h)]	358	360
CO mole fraction emissions	3.1	4.1

As reported by several authors [16, 17], addition of ethanol to gasoline raises the engine volumetric efficiency. Our simulations predict an increase in engine efficiency in the interval from pure isooctane to 12 % ethanol addition from 22.0 % to almost 25.5 %, which amounts a relative improvement of 13.7 %. Although the experimental results report a rather flat efficiency maximum at around 7.5 % ethanol, simulations lead to a smooth increase, and are consistent with the simulation results of Bayraktar [7]. In addition, experiments show a flat maximum for power at about 7.5 % ethanol, but quasi-dimensional simulations predict a monotonically steady increase with the amount of ethanol addition. Differences between the model results and experiments are never more than 6.5 %. Emissions of CO decrease as the volume fraction of ethanol increases. This is a consequence of the fact that ethanol has a lower carbon content than gasoline, and that ethanol addition results in more complete combustion with higher temperatures. Our theoretical predictions on CO emissions are in agreement with the experimental results, although an overestimation of around 25 % is found. With respect to the specific fuel consumption (sfc), addition of ethanol reduces the heating value of gasoline–ethanol blends, and thus in principle, more fuel per unit mass is needed to obtain power outputs similar to those for an engine working with gasoline. But ethanol blends lead to a leaner mixture, therby improving combustion. For these reasons the sfc decreases with an increase in the

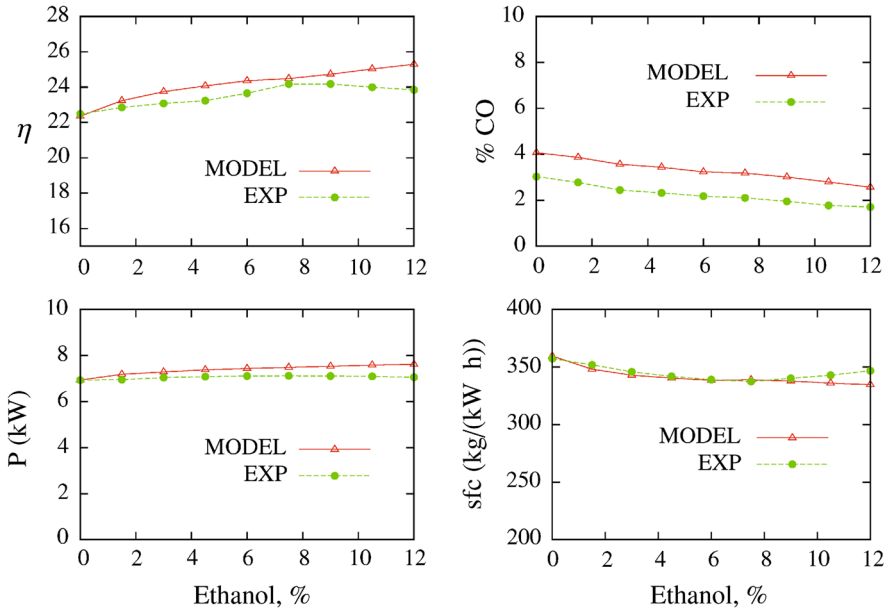

Fig. 1 Comparison of the results from our simulation with the experimental ones of Bayraktar [5]: efficiency (η), power output (P), CO mole fraction emissions, and specific fuel consumption (sfc)

amount of ethanol added. The simulations reveal a more monotonic decrease whereas the experiments exhibit a flat minimum. In any case, numerical differences between the simulated and experimental results are quite small.

In order to study the cycle-to-cycle variations (CCV) in a simulated engine, it is necessary to introduce a stochastic component into the combustion model [26, 34]. As mentioned in the Introduction, there are several sources of CCV including turbulence in the flow field, inhomogeneity of the mixture composition near the spark plug, and memory effects associated with the presence of residual gases in the combustion chamber at the beginning of successive engine cycles [30]. In our combustion model, as we shall discuss below, the laminar speed S_l relates the combustion dynamics with the fraction of residual gases in the cylinder, and so it is associated with the memory of the chemistry of combustion. The essential parameters that characterize the development of combustion are: (a) the characteristic length of eddies, l_t, (b) the turbulent entrainment velocity, u_t, and (c) the location of the ignition kernel. It was shown in [26, 34] that incorporation of stochastic fluctuations in l_t or u_t is basic to reproduce the experimental phenomenology of the cycle-to-cycle variations. By fitting the experimental results for combustion of Beretta [28], we added a stochastic component in l_t, considered as a random variable with a log-normal probability distribution: $logN\left(\mu_{log_{l_t}}, \sigma_{log_{l_t}}\right)$ around the nominal value, $l_t^0 = 0.8 L_{v,max}\left(\frac{\rho_i}{\rho_u}\right)^{3/4}$ with standard deviation, $\sigma_{log_{l_t}} = 0.222$, and mean, $\mu_{log_{l_t}} = log\left(l_t^0\right) - \left(\sigma_{log_{l_t}}^2/2\right)$. The velocity u_t is correlated with l_t from the empirical correlations by Beretta [28]: $u_t = 0.08\overline{u}_i\left(\frac{\rho_u}{\rho_i}\right)^{1/2}$ and $l_t = 0.8 L_{v,max}\left(\frac{\rho_i}{\rho_u}\right)^{3/4}$. In these equations $\overline{u}_i$ represents the mean inlet gas speed, $L_{v,max}$ the maximum intake valve lift, ρ_i the fresh mixture density at ambient conditions, and ρ_u, the density of the unburned gas mixture inside the combustion chamber. From the empirical correlations of Beretta [28] for l_t and u_t, we note that they depend on the mean inlet gas speed and the maximum valve lift, but not on the chemical composition of the mixture. So, the random component for l_t for the isooctane-ethanol mixture [33] is taken to be identical to that for pure isooctane [26]. Details on this procedure and the parameters for the cylinder shape and size and other variables required to run the simulation are given in [26, 34]. Some of the geometrical and other parameters of the simulated engine are listed in Table 1.

3 Results and discussion

We begin by performing a standard statistical analysis of the heat release time series. Our results are obtained

with a time time series of 2000 consecutive cycles after an adequately long equilibration period. In particular, we calculate the mean, standard deviation, and coefficient of variation (COV) of the heat release time series for different equivalence ratios and different volume fractions of ethanol addition. As in many previous studies, the COV is used here as a measure of the CCV in heat release. The COV of a time series is a measure of dispersion of the data with respect to its mean value. For a time series $\{x_i\}$, $i = 1, 2, 3, \ldots, N$, the COV is defined as the ratio of its standard deviation (σ) to its mean value(μ), and is usually expressed in percent form.

$$\mathrm{COV} = \frac{\sigma}{\mu} \times 100\,\%, \tag{6}$$

where

$$\mu = \frac{1}{N}\sum_{i=1}^{N} x_i, \sigma = \left[\frac{1}{N}\sum_{i=1}^{N}(x_i - \mu)^2\right]^{1/2}. \tag{7}$$

The coefficient of variation (COV) is a useful statistic for comparing the degree of variation between two time series even when their mean values are quite different from each other. For a given time series, the COV provides a single overall numerical measure characterizing the temporal variability in the data; however, it does not take into account the spectral characteristics of the time series. We use a wavelet-based approach to describe the spectral-temporal aspects of CCV of the heat release time series, and estimate the effect of ethanol addition on the CCV.

Wavelet-based techniques are being increasingly used for time series analysis in a wide variety of applications. They are particularly useful for the analysis of transient and intermittent processes. We used a continuous wavelet transform (CWT) to analyze the heat release time series. The CWT maps the spectral characteristics of a time series on to a time–frequency (time-period) plane from which the various periodicities and their temporal variations, if any, can be discerned by visual inspection. Using a variable-size window in the time–frequency (time-period) plane, the CWT adjusts the time and frequency resolutions in an adaptive fashion. It uses a window that narrows when focusing on high-frequency components of the time series and widens on low-frequency features, analogous to a zoom lens [35]. Recently, wavelet analysis using CWT has been applied to the analysis of CCV in internal combustion engines by Sen et al. [36–40].

Using CWT, we analyzed the heat release time series obtained from the quasi-dimensional model of Curto-Risso et al. [33] to elucidate the spectral-temporal characteristics of their CCV. In particular, by calculating the wavelet power spectrum (WPS) and global wavelet spectrum (GWS), the dominant oscillatory modes of the CCV are identified, and the engine cycles over which these modes may persist are delineated. On the basis of the dominant periodicities and spectral power, we investigate the effect of ethanol addition on the CCV. In this study, the equivalence ratio (ϕ) is changed from 0.7 to 0.9 and 1.0, i.e., from very lean to stoichiometric, and ethanol is added in the volumetric proportions of 5, 10, and 25 %.

3.1 Statistical Analysis

First we present the results of the standard statistical analysis mentioned above. For the purpose of illustration, we have plotted in Fig. 2 the heat release time series for the equivalence ratio: $\phi = 0.7$, with ethanol added from 0 to 25 % by volume. For brevity, the heat release time series for other values of the equivalence ratio examined here are not shown. Notice that the heat

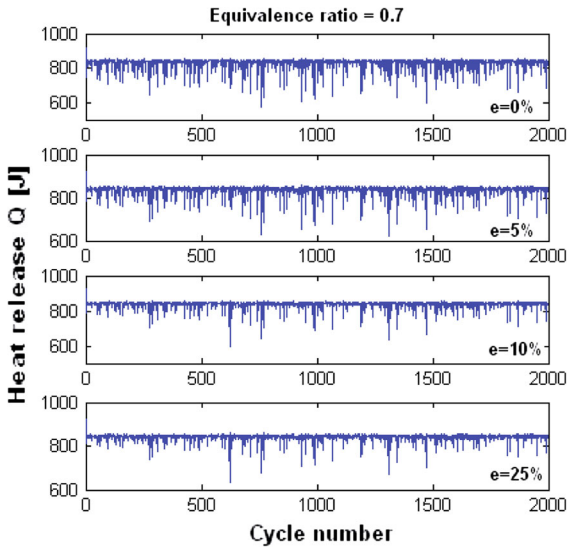

Fig. 2 Heat release time series of the simulated spark ignition engine for the equivalence ratio $\phi = 0.7$, and ethanol added in the amounts: e = 0, 5, 10, and 25 % by volume

release time series in Fig. 2 exhibits varying degrees of intermittency. A common feature of all time series in this figure is that they are quite asymmetric: abundant combustion events leading to a poor heat release. Previous experimental [41] and simulation results [26] showed this fact for engines working with pure isooctane. In order to visualize the effect of ethanol addition on the importance of CCV, in Fig. 3, we show how the (a) mean, and (b) COV of the heat release time series change with changes in the amount of ethanol added, for fixed values of the equivalence ratio: $\phi = 0.7$, 0.9, and 1.0.

Consider Fig. 3a. It is apparent from this figure that for a fixed equivalence ratio (ϕ), the mean value of the heat release is almost insensitive to changes in the volume fraction of ethanol added, except when the combustible mixture is very lean ($\phi = 0.7$). In this case, the mean heat release value increases slightly with an increase in ethanol content, especially between 0 and 5 %. In addition, we see from this figure that at a fixed ethanol fraction, the mean value of the heat release decreases as ϕ decreases, i.e., the mixture becomes leaner.

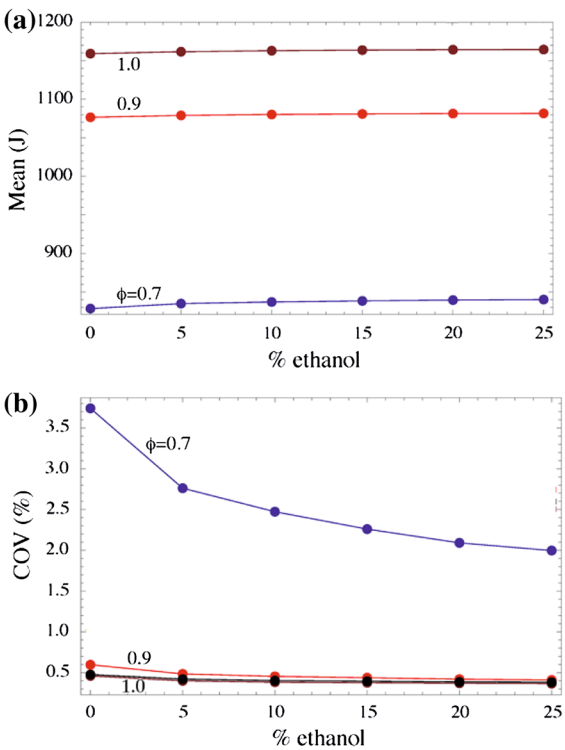

Fig. 3 Changes in **a** mean and **b** coefficient of variation (COV) of the heat release time series as a function of the percent volume of ethanol added, for the equivalence ratios: $\phi = 0.7$, 0.9, and 1.0

Next we consider Fig. 3b which shows the changes in the coefficient of variation (COV) of the heat release time series with changes in ethanol content for the three equivalence ratios considered above. It is clear that for each equivalence ratio, the COV decreases as the volume fraction of ethanol increases. It is worth pointing out that for any ϕ, the addition of 5 % of ethanol leads to a decrease of around 30 % in the COV. Higher ethanol percentages progressively diminish COV, but to a lesser extent.

It is also apparent from Fig. 3b that the COV is, in general, greater for leaner mixtures. In addition, we observe that for a stoichiometric mixture ($\phi = 1.0$), the COV reaches a minimum for all ethanol fractions, implying that the cycle-to-cycle heat release variations are the smallest when the mixture is stoichiometric.

3.2 Wavelet analysis

We have analyzed the above heat release time series using a continuous wavelet transform (CWT). The analysis methodology of CWT has been described in detail by Torrence and Compo [42]. We summarize the main steps below. A mother wavelet is chosen and its convolution with the time series signal is computed. This convolution is defined as the CWT of the time series. The CWT is computed by manipulating the mother wavelet over the time series in two ways: it is moved to various locations on the time series, and it is stretched or squeezed. If the wavelet locally matches the shape of the time series, then a large transform value is obtained. If, on the other hand, the wavelet and the time series do not correlate well, a low value of the transform will result [42]. The squared modulus of the CWT, representing the signal energy, is defined as the wavelet power spectrum (WPS). The WPS is plotted on a time–frequency (or time-period) plane, which depicts the various periodicities of the time series and their temporal variations. For the heat release time series considered here, the WPS is plotted on a plane with the cycle number and period (cycle) as the two axes. From the WPS, another useful quantity called the global wavelet spectrum (GWS) can be computed. The GWS is the average of the WPS over all time, and is analogous to a smoothed Fourier spectrum. From the locations of the peaks in the GWS, the dominant periodicities of the time series can be identified. In our

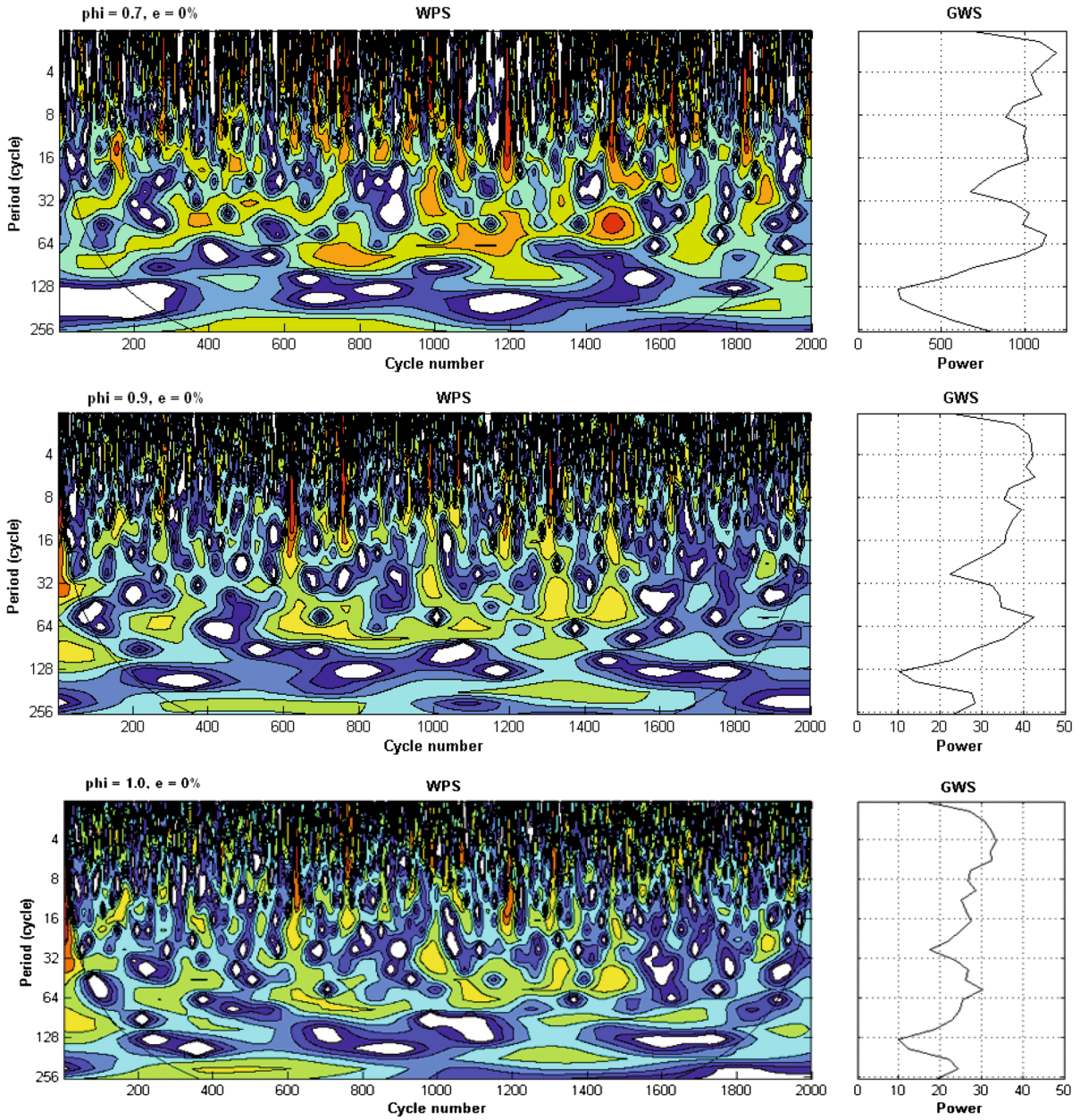

Fig. 4 Wavelet power spectrum (WPS) and global wavelet spectrum (GWS) of the heat release time series of the simulated spark ignition engine fueled by gasoline (with no ethanol added) for equivalence ratios: $\phi = 0.7$, 0.9, and 1.0

analysis, we used a Morlet wavelet of order 6 as the mother wavelet. This choice provides a good balance between the time and frequency resolutions. The Morlet wavelet has been used as a mother wavelet in a variety of applications. Convergence of the wavelet results were performed using the methodology described in [42]. It was found that the data with 2000 consecutive cycles was adequate to capture the low frequency cycles in the heat release time series. The interested reader is referred to [42] for further methodological details. In this work, we used the amplitude of the GWS to estimate the effect ethanol addition on CCV. In particular, as shown below, addition of ethanol leads to a reduction in the

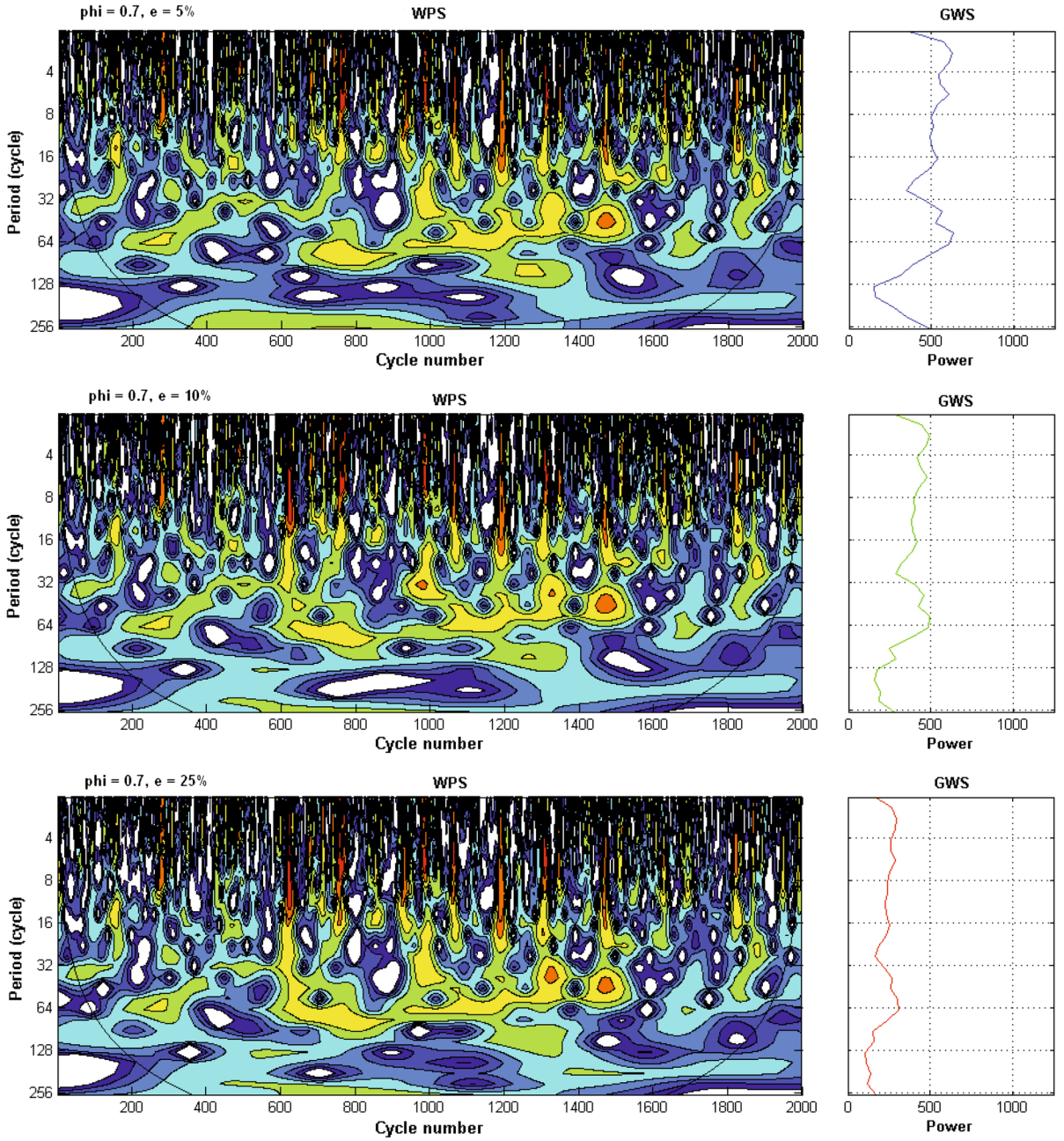

Fig. 5 Wavelet power spectrum (WPS) and global wavelet spectrum (GWS) of the heat release time series of the spark engine with equivalence ratio of 0.7, and ethanol added in the amounts 5, 10, and 25 % by volume

amplitude of the GWS, indicating that ethanol addition reduces the cyclic variability of the heat release in the gasoline engine fueled by gasoline–ethanol blends.

First we apply a CWT to the heat release time series for a gasoline engine (with no ethanol added), and investigate the effect of changing the equivalence ratio (ϕ) on the cycle-to-cycle variations. The equivalence ratio is changed from $\phi = 0.7$ and 0.9 for lean mixtures, to $\phi = 1.0$ for a stoichiometric mixture. Figure 4 illustrates the WPS and GWS of the various

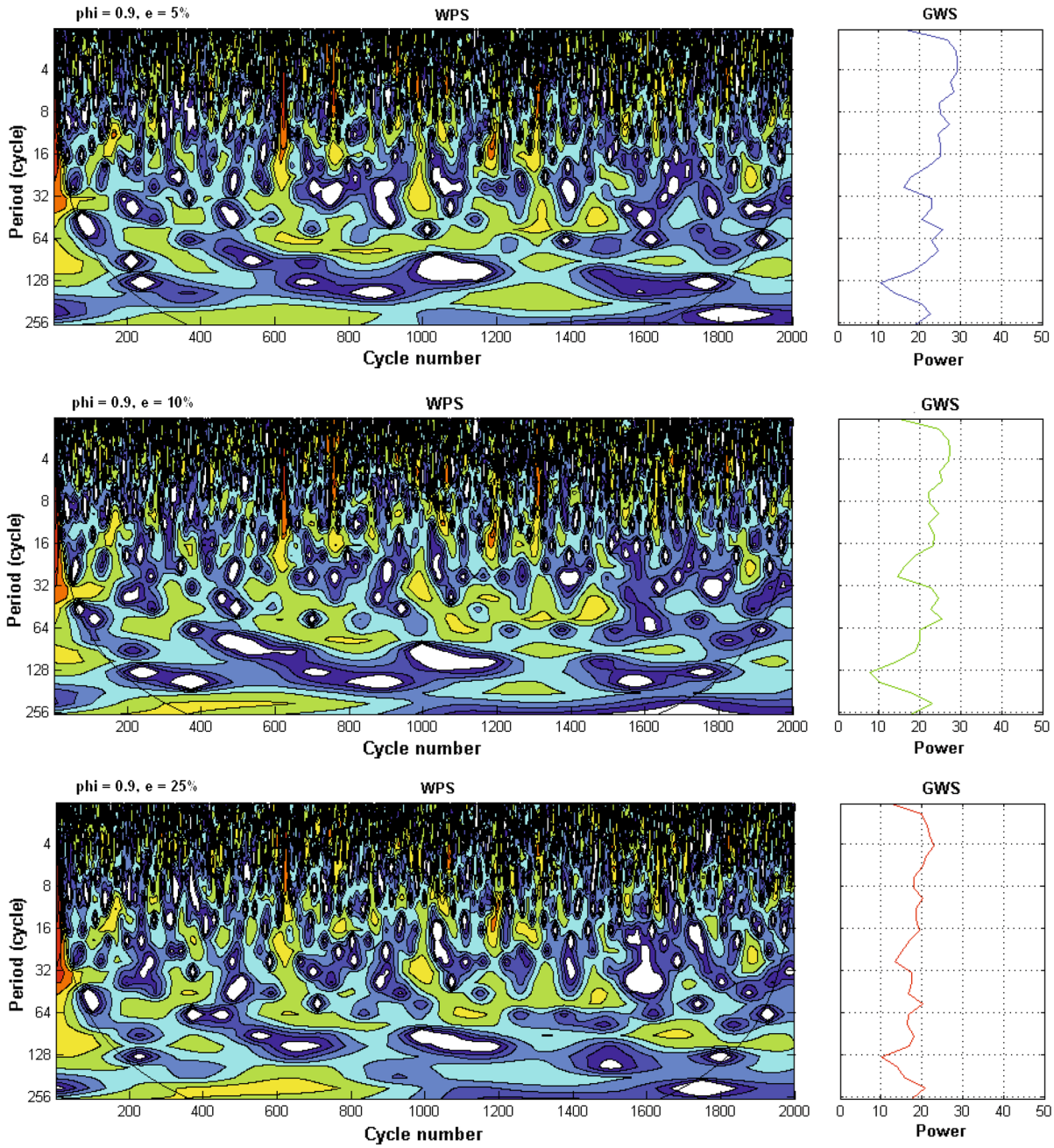

Fig. 6 Wavelet power spectrum (WPS) and global wavelet spectrum (GWS) of the heat release time series of the spark engine with equivalence ratio of 0.9, and ethanol added in the amounts 5, 10, and 25 % by volume

time series. In the WPS, the colors red and blue represent high and low power, respectively, with the other colors designating intermediate power levels. The area below the U-shaped curve represents the cone of influence (COI). For the computation of the WPS, the time series is padded with zeros at both ends. The zero padding leads to edge effects which make the WPS inside the COI unreliable; the WPS inside the COI should therefore be used with caution [40]. Consider the WPS shown in the top panel of Fig. 4,

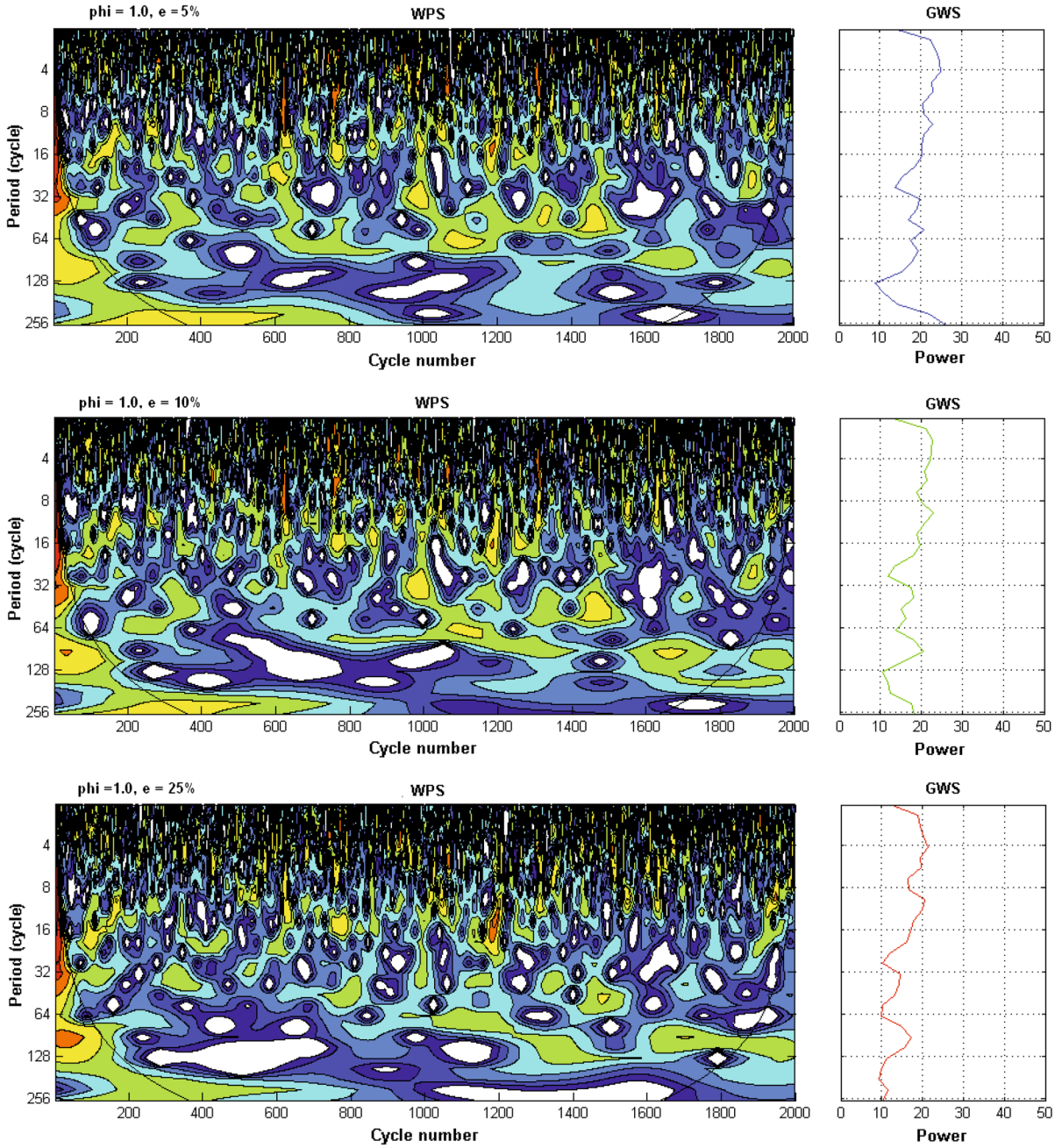

Fig. 7 Wavelet power spectrum (WPS) and global wavelet spectrum (GWS) of the heat release time series of the spark engine with equivalence ratio of 1.0 and ethanol added in the amounts 5, 10, and 25 % by volume

which applies to $\phi = 0.7$. This figure shows the presence of both high-frequency (low-period) intermittent fluctuations and more persistent low-frequency variations in the heat release time series. Intermittency is characterized by sudden bursts of power separated by intervals of very low power or almost quiescent intervals. The low-frequency variations are most dominant around the 56-cycle period and persist over several engine cycles. The dominant periodicities with corresponding peaks can be

discerned from the GWS shown on the right.

Next we consider the results for $\phi = 0.9$. The WPS and GWS for this case are depicted in the middle panel of Fig. 4. As in the WPS for $\phi = 0.7$ (upper panel), this WPS also shows high frequency intermittent fluctuations and low frequency variations, but a comparison of the GWS in this panel and the top panel reveals that the overall spectral power is significantly reduced. The WPS and GWS for a stoichiometric mixture ($\phi = 1.0$) are presented in the bottom panel in Fig. 4. Both high frequency intermittency and low frequency periodicities are also seen in this WPS, and the GWS in this figure indicates an additional reduction in the overall spectral power implying that the cycle-to-cycle heat release variations are further diminished.

We now examine the cyclic variability of heat release in a spark-ignition engine fueled by gasoline–ethanol blends. Figure 5 depicts the WPS and GWS of the heat release time series for the lean mixture with $\phi = 0.7$, and ethanol volume fractions of 5, 10, and 25 %. As in the case of the gasoline engine with no ethanol addition, the WPS in each of the three panels in this figure shows the presence of both high-frequency (low-period) intermittent fluctuations and more persistent low-frequency variations. Furthermore, the GWS plots in the three panels indicate that the overall spectral power progressively decreases with increase in ethanol content. This is in accordance with the decreasing of CCV effects in terms of the COV as seen in Fig. 3(b). Figures 6 and 7 present the WPS and GWS for $\phi = 0.9$, and 1.0, respectively. The WPS plots in this figure show the occurrence of high-frequency intermittent fluctuations; however, the low-frequency variations are less persistent and rather intermittent in nature. In addition, from the GWS in each of the Figs. 6 and 7, we see that the overall spectral power tends to decrease with an increase in ethanol content.

4 Concluding remarks

We have analyzed the cycle-to-cycle variations (CCV) of heat release in a simulated spark ignition engine fueled by gasoline–ethanol blends. The CCV were analyzed using the coefficient of variation (COV) and a continuous wavelet transform (CWT). The results based on the COV reveal that for a fixed equivalence ratio, the CCV decrease significantly as the ethanol content is increased, when the combustible mixture is very lean. When the mixture is close to stoichiometric, the decrease of the CCV is not sensitive to a change in ethanol content. In addition, the COV results show that for a fixed ethanol content, the CCV decreases with an increase in equivalence ratio, and this increase is more pronounced for leaner mixtures. The results of wavelet analysis indicate that the CCV of heat release in a spark ignition engine fueled by gasoline an gasoline–ethanol blends exhibit multiscale dynamics consisting of high frequency intermittent fluctuations and low frequency oscillations. For a gasoline engine (with no ethanol added), the CCV are reduced as the composition of the combustible mixture goes from fuel-lean toward stoichiometric. In addition, for a fixed equivalence ratio, the CCV can be reduced by blending gasoline with ethanol.

In this study, the heat release time series of the simulated spark ignition engine was analyzed over 2000 engine cycles. An advantage of using a model engine is that the model simulations can be easily extended to a larger number of engine cycles. By performing wavelet analysis of longer time series, it would be possible to detect the presence of lower frequencies or long-term variations in the CCV. A longer time series will also enable us to determine if the periodicities identified here will persist over a longer time interval, i.e., more engine cycles.

Acknowledgments We acknowledge the financial support from MICINN of Spain under Grant FIS2010-17147. P.L.C.-R. also acknowledges the support from Universidad de Salamanca, Spain, and Universidad de la República, Montevideo, Uruguay, for his visits to Salamanca.

References

1. Poulton ML (1999) Alternative fuels for road vehicles. Computational Mechanics Publications, Bellerica, MA
2. Kowalewicz A, Wojtyniak M (2005) Alternative fuels and their application to combustion engines. Proc Inst Mech Engrs Part D J Auto Eng 219:103–125
3. Hsieh WD, Chen RH, Wu TL, Lin TH (2002) Engine performance and pollutant emission of an SI engine using ethanol-gasoline blended fuels. Atmos Environ 36:403–410
4. He BQ, Wang JX, Hao JM, Yan XG, Xiao JH (2003) A study on emission characteristics of an EFI engine with ethanol-blended gasoline fuels. Atmos Environ 37:949–957
5. Al-Hassan M (2003) Effect of ethanol-unleaded gasoline blends on engine performance and exhaust emissions. Energy Convers Manage 44:1547–1561

6. Yüksel F, Yüksel B (2004) The use of ethanol-gasoline blend as fuel in an SI engine. Renew Energy 29:1181–1191
7. Bayraktar H (2005) Experimental and theoretical investigation of using gasoline–ethanol blends in spark ignition engines. Renew Energy 30:1733–1747
8. Ceviz MA, Yüksel F (2005) Effect of ethanol-unleaded gasoline blends on cyclic variability and emissions in an SI engine. Appl Therm Eng 25:917–925
9. Bayraktar H (2007) Theoretical investigation of flame propagation process in an SI engine running on gasoline–ethanol blends. Renew Energy 32:758–771
10. Young MB (1981) Cyclic dispersion in a homogeneous charge spark ignition engine: a literature survey. SAE paper No. 810020
11. Heywood JB (1988) Internal combustion engine fundamentals. McGraw Hill, New York
12. Sztenderowicz ML, Heywood JB (1990) Cycle-to-cycle heat release fluctuations in a stoichiometrically fueled SI engine at low speed and load. SAE Paper 902143
13. Daw CS, Finney CEA, Kennel MB, Connolly FT (1997) Cycle-by-cycle combustion variations in spark-ignited engines. Proceedings of the fourth experimental chaos conference, Boca Raton, Florida USA
14. Fujikawa T, Nomura Y, Hatton Y, Kobayashi T, Kanda M (2003) Analysis of cycle-by-cycle variation in a direct injection gasoline engine using a laser-induced fluorescence technique. Int J Engine Res 4:143–153
15. Stone CR, Brown AG, Beckwith P (1996) Cycle-to-cycle variations in spark ignition engine combustion: Part II: modeling of flame kernel displacements as a cause of cycle-to-cycle variations. SAE Paper 960613
16. Scholl D, Russ S (1999) Air-fuel ratio dependence of random and deterministic cyclic variability in a spark ignition engine. SAE Paper 1999-01-3513
17. Galloni E (2009) Analyses about parameters that affect cyclic variation in a spark ignition engine. Appl Therm Eng 29:1131–1137
18. Ozdor N, Dulger M, Sher E (1994) Cyclic variability in spark ignition engines: a literature survey. SAE Paper No. 940987
19. Ishii K, Sasaki T, Urata Y, Yoshida K, Ohno T (1997) Investigation of cyclic variation of heat release under lean burn operation in spark ignition engines. SAE Paper 972830
20. Zervas E (2004) Correlations between cycle-to-cycle variations and combustion parameters of a spark ignition engine. Appl Therm Eng 24:2075–2081
21. Zheng J, Huang Z, Wang J, Wang B, Ning D, Zhang Y (2009) Effect of compression ratio on cycle-by-cycle variations in a natural gas direct injection engine. Energy Fuels 23:5357–5366
22. Gülder PI (1984) Burning velocities of ethanol-isooctane blends. Combust Flame 56:261–268
23. Tatschl R, Wieser K, Reitbauer R (1994) Multidimensional simulation of flow evolution, mixture preparation and combustion in a 4-valve SI engine. In: international symposium COMODIA 94, Yokohama
24. Vermorel O, Richard S, Colin O, Angelberger C, Benkenida A (2007) Predicting cyclic variability in a 4-valve SI engine using LES and the AVBP code. International multidimensional engine modeling user's group meeting
25. Lacour C, Pers C, Enaux O, Vermorel G, Angelberger C, Poinsot T (2009) Exploring cyclic variability in a spark ignition engine using experimental techniques, system simulation and large-eddy simulation. In: European Combustion meeting
26. Curto-Risso P, Medina A, Calvo-Hernández A, Guzman-Vargás L, Angulo-Brown F (2011) On cycle-to-cycle heat release variations in a simulated heat engine. Appl Energy 88:1557–1567
27. Blizard NC, Keck JC (1974) Experimental and theoretical investigation of turbulent burning model for internal combustion engines. SAE Paper 740191
28. Beretta GP, Rashidi M, Keck JC (1983) Turbulent flame propagation and combustion in spark ignition engines. Combust Flame 52:217–245
29. Shen F, Hinze P, Heywood JB (1996) A study of cycle-to-cycle variations in SI engines using a modified quasi-dimensional model. SAE Paper 961187
30. Abdi Aghdam E, Burluka AA, Hatrell T, Liu K, Sheppard GW, Neumeister, Grundwell N (2007) Study of cyclic variation in an SI engine using a quasi-dimensional model. SAE paper 2007-01-0939
31. Curto-Risso P, Medina A, Calvo-Hernández A (2008) Theoretical and simulated models for an irreversible Otto cycle. J Appl Phys 104:094911
32. Curto-Risso P, Medina A, Calvo-Hernández A (2009) Optimizing the operation of a spark ignition engine: simulation and theoretical models. J Appl Phys 105:094904
33. Curto-Risso PA, Medina A, Calvo-Hernández A (2011) Effect of gasoline–ethanol blends on cycle-to-cycle variability. In 24th international conference on efficiency, cost, optimization, simulation and environmental impact, Novi Sad, Serbia, July 4–7, 2011; ECOS 2011
34. Curto-Risso P, Medina A, Calvo-Hernández A (2010) Monofractal and multifractal analysis of simulated heat release fluctuations in a spark ignition engine. Phys A 389:5662–5670
35. Kumar P, Foufoula-Georgiou E (1997) Wavelet analysis for geophysical applications. Rev Geophys 35:385–412
36. Sen AK, Longwic R, Litak G, Gorski K (2008) Analysis of cycle-to-cycle pressure oscillations in a diesel engine. Mech Syst Signal Process 22:362–373
37. Sen AK, Litak G, Edwards KD, Finney CEA, Daw CS, Wagner RM (2011) Characteristics of cyclic heat release variability in the transition from spark ignition to HCCI in a gasoline engine. Appl Energy 88:1648–1655
38. Sen AK, Litak G, Yao BF, Li GX (2010) Analysis of pressure fluctuations in a natural gas engine under lean burn conditions. Appl Therm Eng 30:776–779
39. Sen AK, Zheng J, Huang Z (2011) Dynamics of cycle-to-cycle variations in a natural gas direct-injection spark ignition engine. Appl Energy 88:2324–2334
40. Sen AK, Ash SK, Huang B, Huang Z (2011) Effect of exhaust gas recirculation on cycle-to-cycle variations in a natural gas spark ignition engine. Appl Therm Eng 31:2247–2253
41. Sen AK, Litak G, Finney C, Daw C, Wagner R (2010) Analysis of heat release dynamics in an internal combustion engine using multifractals and wavelets. Appl Energy 87:1736–1743
42. Torrence C, Compo GP (1998) A practical guide to wavelet analysis. Bull Am Meteorol Soc 79:61–78